POLITECNICO DI TORINO
Repository ISTITUZIONALE

A new framework to estimate the probability of fire following earthquake

(Article begins on next page)

16 July 2022

2c-0191

A NEW FRAMEWORK TO ESTIMATE PROBABILITY OF FIRE FOLLOWING EARTHQUAKE

S. Marasco[1], A. Zamani Noori[2], A. Cardoni[3], M. Domaneschi[4], G.P. Cimellaro[5]

[1] *Postdoctoral research associate, Department of Structural, Geotechnical and Building Engineering, Politecnico di Torino, Italy, email: sebastiano.marasco@polito.it*
[2] *Postdoctoral research associate, Department of Structural, Geotechnical and Building Engineering, Politecnico di Torino, Italy, email: ali.zamani@polito.it*
[3] *PhD student, Department of Structural, Geotechnical and Building Engineering, Politecnico di Torino, Italy, email: alessandro.cardoni@polito.it*
[4] *Assistant professor, Department of Structural, Geotechnical and Building Engineering, Politecnico di Torino, Italy, email: marco.domaneschi@polito.it*
[5] *Associate professor, Department of Structural, Geotechnical and Building Engineering, Politecnico di Torino, Italy, email: gianpaolo.cimellaro@polito.it*

Abstract

Fire following earthquake has been recognized as a very significant risk in the past decade. Several studies have been performed by researchers to develop analytical and experimental methods to assess the economic and life losses due to fire after an earthquake event. While the outcome of these efforts has resulted in significant advances, an accurate and simplified framework to be utilized by practicing engineers is still lacking. In this paper, a new methodology to predict the probability to have fire following a seismic event considering the building seismic damage is proposed. Earthquake was considered as the main hazard, whereas blast and fire were assumed as a cascading hazards. Bayesian approach was used to estimate conditional probability of fire caused by an earthquake. A hospital building has been assumed as case study, while a LPG tank located nearby the structure has been considered as potential source of blast and ignition. A physical-based simulation was used to evaluate intra-structure ignition probability due to leakage and/or breaks of the gas pipelines. Several parameters were considered to model the occurrence of intra-structure ignitions such as structural and non-structural damage, earthquake intensity, buildings geometry and occupancy and earthquake scenario time. proposed framework is considered a significant step to accurately predict fire risk following a seismic event with affordable time and it can be an alternative solution to the statistical ignition model currently being used in many fire following hazard methods.

Keywords: fire; earthquake; ignition probability; building damage, FFE, multi hazard,

1. Introduction

Large parts of the world are subjected to multiple natural, manmade, and artificial hazards. The rising of global population and the massive economic development in areas prone to disasters have increased the chance of multiple catastrophic incidents, which lead to disruption of buildings and infrastructures. Therefore, multiple-hazard engineering and related mitigation risks play a key role in design and retrofitting of buildings.

Multiple-hazard analysis has been defined as the "implementation of methodologies and approaches aimed at assessing and mapping the potential occurrence of different types of natural hazards in a given area. The employed methods have to take into account the characteristics of the single hazardous events as well as their mutual interactions and interrelations"[1] The multiple-hazard assessment has to be performed by comparing risks of cascading mechanisms related to triggered hazard events [2]. For instance, the impact of an earthquake on a gas pipeline can initiate gas leakage, which may likely cause an explosion. There are several examples of sequential hazards initiated by an earthquake which have caused fire such as San Francisco (1906), Tokyo (1923), Kobe (1995), Northridge (1994), and Japan (2011) earthquakes.

The risk assessment of structures that are exposed to more than one hazard are determined by adopting the performance-based approach. For example, Barbato et al. (2013) [3] suggested a novel assessment method that involved the evaluation of the individual impacts of the interaction among hurricane wind, flood, windborne debris, and rainfall hazards in the Performance-Based Hurricane Engineering (PBHE) framework.

Multiple-hazard design starts with the structural and non-structural analysis for individual hazard. The location, magnitude and frequency of occurrence of each hazard have to be estimated through a probabilistic approach. Several probabilistic approaches have been proposed for multiple-hazard risk assessment. Asprone et al. (2010) [4] assessed the blast damage for a four-story reinforced concrete building in addition to seismic fragility. A possible blast scenario has been assumed during the service life of a building located in a seismic zone, and then the probability of progressive collapse has been calculated using a Monte Carlo simulation procedure. A quantitative risk analysis of industrial facilities in a seismic area has been carried out by Fabbrocino et al. (2005) [5] taking properly in account the multiple-hazard effects. An oil storage plant with several atmospheric steel tanks containing flammable materials has been considered as case study. The vulnerability of the steel tanks has been estimated through a quantitative probabilistic seismic risk analysis. The response of the industrial equipment has been expressed in terms of limit states defined in accordance with the post-earthquake damage observations and the consequence analysis has been performed.

In this paper, a new approach to estimate the total amount of structural damage caused by sequential hazard is proposed. Earthquake, blast and fire have been considered as sequential hazards and numerical analyses have been performed to assess the fragility functions for each hazard. The combination of the structural damage for sequential hazards is evaluated according to Bayes' theorem. The conditional probability of sequential hazard occurrence is estimated by using physical models that takes into account the vulnerability of a structural component in reference to a given hazard. The methodology has been applied to a steel structure hospital located in California, US [6, 7]. The first section of the paper provides a detailed description of the proposed methodology, while the second part illustrates its applicability through a case study building.

2. Methodology

The implementation of multi-hazard approach may be applied in order to improve the safety of structures and minimize life cycle costs and human losses. In the Performance-Based framework the structural vulnerability is conventionally expressed in terms of probability to exceed a stated performance objective when the structure is subjected to a certain level of hazard. In case of sequential hazardous events, the probabilistic correlation between the main hazard and the occurrence of the other hazards has to be estimated to assess the performance of the structural system. In the proposed methodology, the occurrence of a sequential hazard for a given Intensity Measure (IM) of the main hazard is estimated following a probabilistic Bayesian approach. The estimation of the conditional probability that one hazardous event occurs as consequence of another hazard is provided by using specific physical models.

As example, a steel tank containing flammable materials in a seismic zone is considered. The probability to have the explosion of the tank due to an earthquake with a given intensity is strictly dependent on (*i*) mechanism of ignition of the material inside the tank, and (*ii*) failure modes and equipment damage of the tank. A physical model has to be capable to describe the fragility of the tank with reference to the possible trigger of the hazardous mechanism. Identifying the most probable failure mode and modeling the geometry of the tank, a numerical analysis has to be performed to evaluate the blast fragility of the tank. In order to take into account different earthquake scenario, several numerical analyses have to be carried out. According to the mechanism of ignition, a maximum threshold of the earthquake response parameter of the tank has to be fixed. When this maximum limit is exceeded, the probability to have explosion is equal to 1, and 0 otherwise. The probability to have explosion after earthquake is obtained by lognormal fitting of the results. This simple procedure is able to provide a conditional probability of explosion due to earthquake for different seismic intensity.

The vulnerability of a structural system to a hazard is expressed in terms of fragility functions derived from numerical analyses for a given damage state. In a multiple-hazard scenario, the prediction of the level of structural damage has to take into account the chain effects. They represent the modification of the structural characteristics caused by the previous hazard. Therefore, the sequential hazards are treated as depend phenomena. The cumulative damage probability due to sequential hazardous events (*P(DS<ds)*) is expressed as product between conditioned probability of the sequential events and the exceedance damage probability for single hazard. Eq. (1) generally gives the cumulative probability to exceed a specified level of damage according to the proposed methodology.

$$P(DS > ds) = P(DSH1 > dsh1 \mid SP0) + P(DSH2 > dsh2 \mid SP1) \cdot P(H2 \mid H1) + P(DSH3 > dsh3 \mid SP2) \cdot P(H3 \mid H2) \cdot P(H2 \mid H1) + ...$$
$$for : 0 \leq P(DS > ds) \leq 1$$

(1)

where H_1, H_2 and H_3 represent three sequential hazards while $P(DSH_1<dsh_1|SP_0)$, $P(DSH_2<dsh_2|SP_1)$ and $P(DSH_3<dsh_3|SP_2)$ are the exceedance damage probability for the considered hazards. The variability in the structural parameters is expressed by the structural system parameters SP_0, SP_1 and SP_2 that consider the chain effects.

A five-story steel hospital building with dimension in plan of 82.3 m by 33.7 m, spans length of 9.1 m and 12.3 m, and the story height equal to 4.6 m is considered. The building has two external lateral moment resisting frames in the longest direction and bracing system in the other direction. The H sections (wide channel, W) have been used for beams (24x55) and columns (12x52) while hollow structural sections (HSS, 10x10x1/4) have been designed for bracing system. The building is situated in Oakland, California, US (Lat: 37.7792, Long: -122.1620). An additional source of electricity is provided, just in case of an unexpected power outage. It includes an aboveground LPG tank equipped of power sources, controls, transfer equipment, supervisory equipment and accessory situated outside the building. The tank has the capacity to generate 2500 kVA of electricity for 8 hours. The LPG tank has a total capacity of 3597 litres and it is located 9.2 m far from the building.

3. Hazard analysis

Earthquake (main hazard), blast and fire have been assumed as sequential hazards. The sequence of hazards caused by the earthquake is not specified and depends on the localization of the high risk potential elements inside and outside the structure as well as their fragility. Logical tree of multi-hazard sequence for general healthcare facilities is represented in Fig 1.
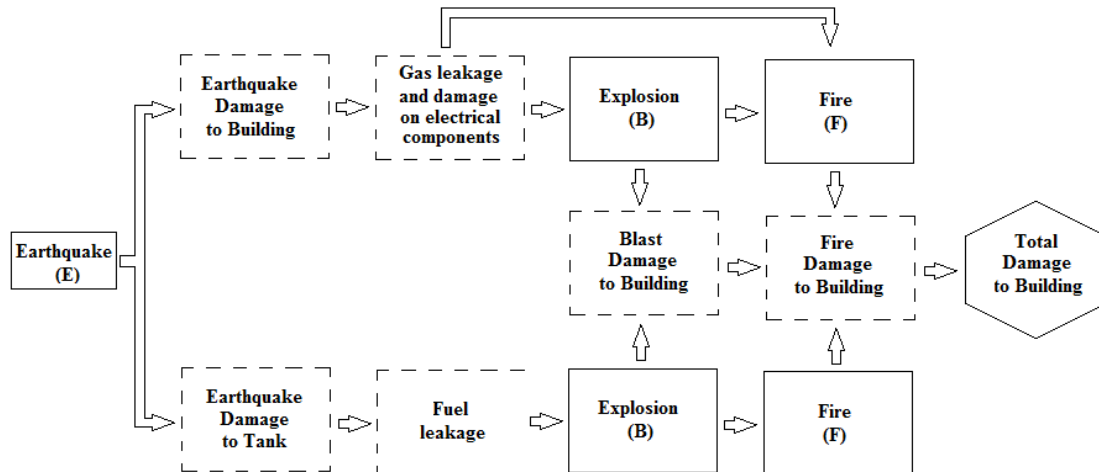

Fig 1 – Hazard sequence: earthquake-blast-fire

The external fuel tank and building elements are both damaged by the earthquake. The fuel leakage can cause an ignition that results in a deflagration of the fuel inside the tank. This series of events may cause explosion of the tank and generate an impulsive air pressure load on the front face of the building. The heat of the gas explosion may also ignite any inflammable materials located within the buildings. In a short time the ignition generates flashover and fire propagates thorough the building compartment.

Fragility curves for each hazard have been derived considering earthquake (*P(DE>de)*), blast (*P(DB>db)*), and fire (*P(DF>df)*) hazard. For this case study, the cumulative probability to exceed a specified level of damage is expressed in Eq. (2).

$$P(DS > ds) = P(DE > de) + P(DB > db) \cdot P(B \mid E) + P(DF > df) \cdot P(F \mid B) \cdot P(B \mid E)$$
$$for : 0 \le P(DS > ds) \le 1$$
(2)

Post-earthquake effects on the small size tanks have shown a low fragility of these elements. Thus, the associated probability to have an explosion and the associated damage exceedance probability is strongly reduced. For this reason, the proposed methodology has been applied neglecting the chain effects.

3.1 Earthquake hazard analysis

Five different Hazard Levels (HL) have been identified (50%, 20%, 10%, 5%, and 2% of exceedance probability in 100 years) and analyses for each of the levels have been conducted. The mean value of moment magnitude ($M_{W,mean}$) and epicenter distance (R_{mean}) with the logarithmic spectral offset at reference period ($\varepsilon(T_{ref})$) have been evaluated according to Boore-Atkinson attenuation law [8] for each HL. All the data can be found through the interactive de-aggregation of USGS (http://geohazards.usgs.gov/deaggint/2008/).

A new Ground Motion Selection and Modification (GMSM) procedure has been used to minimize the dispersion values of the Engineering Demand Parameter (EDP) calculated through dynamic analyses. The first period of the structure has been selected as conditioning period (T_{ref}). The five target spectra and the associated spectrum-compatible groups of ground motions have been obtained through the software

2c-0191

OPENSIGNAL 4.1 [9]. Parts of the results in terms of mean spectrum-compatibility have been illustrated in Fig 2. Moreover, the spectral acceleration at reference period has been considered as Intensity Measure (IM).
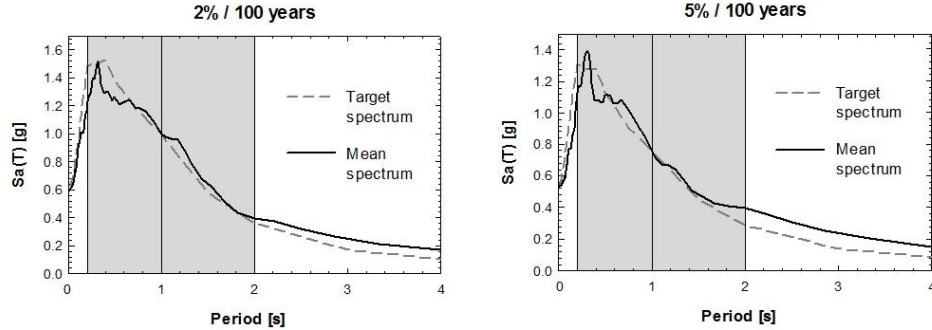

Fig 2 – Mean spectrum compatibility for the five HLs

3.2 Blast hazard analysis

After earthquake, the power supplier system (fuel tank, electrical components, etc.) may be slightly or severely damaged. A fuel leakage may be as a result of damaged valves, connections or pipes of a fuel tank. However, an explosion cannot occur when there is not ignition source and when the fuel concentration is less the flammable concentration range. Thus, explosion are usually determined by concentration of fuel, gas leakage and ignition source. Considering the three parameters as stochastic variables, the probability of explosion after earthquake (*P(B/E)*) of a damaged fuel tank is reported in Eq. (3).

$$P(B\,|\,E) = P_L \cdot P_{FC} \cdot P_I \tag{3}$$

where P_L represents the probability of fuel leakage, P_{FC} is the probability to have maximum fuel concentration and P_I defines the probability of ignition. In this case study, it has been assumed that the damage takes place on the pipe that is connected to the tank. This assumption is based on the fact that the tank has a small size. According to ATC P-58 [10] the probability to have large gas leakage for small diameter piping system (*D<10* cm) is given in terms of fragility function with accelerations as EDP (*μ=1.1g, β=0.5*). The probability to have maximum gas concentration has been estimated considering the failure of the pipe closeness to the joint connection. A simplified dynamic model has been developed to predict the maximum horizontal drift of the pipe. The tank has been considered as rigid body, while its legs have been assumed having shear flexibility in horizontal direction. The anchor bolts have been designed according to UBC-97 [11] in order to ensure full restraint at the base. The first period of the tank (*T_tank*) has been calculated considering different fuel quantity as HL (5%, 10%, 20%, 30%, 40%, 50%, 60%, 70%, 80%, 90%, 95%, and 100%). The occurrence of shear failure in the vertical pipe causes the maximum gas concentration. Based on this postulation and considering the maximum shear stress value on the cross section of the pipe, the failure spectral acceleration has been calculated (Eq. (4)).

$$S_{a,failure} = \frac{45.44}{g} \cdot \left(\frac{f_{u,d}}{E} \right) \cdot \left[\frac{L_v^3}{(D_e^2 - D_i^2)(D_e^2 + D_e \cdot D_i + D_i^2)} \right] \cdot \frac{1}{T_{tank}^2} \tag{4}$$

where $f_{u,d}$ and E represent the ultimate stress and elastic modulus of the steel, respectively, D_e and D_i are the external and internal pipe diameter, and L_v is the length of the vertical pipe. The occurrence of maximum gas concentration is recorded when the spectral acceleration of the selected ground motion exceeds the $S_{a,failure}$. In these cases, the probability to have maximum gas concentration has been assumed equal to 1 and 0 otherwise. Then, a tridimensional fragility curve has been developed by fitting a lognormal

5

distribution of the data for each value of fuel quantity (IM_1) and spectral acceleration at period of the tank (IM_2). The ignition probability is provided with reference to the maximum fuel quantity. The information required for risk data assessment is provided by the International Association of Oil and Gas producers [12] in order to evaluate the probabilities of hydrocarbon releases igniting. In this case study, only delayed ignition probability has been considered, since immediate ignition needs sources close to the fuel leakage point. Release of flammable gases from small onshore LPG plant has been assumed as ignition scenario and the related probability function has been derived. The Bernoulli's principle is used for the computation of maximum gas concentration ($FC_{max}=29.70 \ kg/s$). Fig 3.a illustrates the probability to have explosion after earthquake.

3.3 Fire hazard analysis

The probability to have fire inside the building is related to the heat transmission due to the tank explosion. The Stefan Boltzmann's law has been used to compute the heat flux for each point of the building in front of the tank. The twelve different tank fuel quantities have been assumed as first IM (IM_1). The temperature at which LPG burns has been assumed to be 2300 K°, while the atmospheric transmissivity coefficient has been fixed to 0.66. The transfer configuration factor has been calculated for the entire external panel of the building (meshed with 0.5×0.5m elements). The computation of the heat flux on building façade has been accomplished with the help of a Matlab code [13]. Supposing the external panel as fireproof, only the opening surfaces (windows, doors, etc.) have been considered as susceptible to trigger fire inside the building. The minimum value of heat flux that can cause flammable materials in a room to burst into flames has been assumed equal to 30 MJ/m^2.

Comparing the façade of the building with the heat flux map, the starting fire surface has been deduced for each fuel quantity value. The estimated conditional probability to have ignition of elements inside the building has been fixed to 1 whether the maximum heat flux on the opening is greater than the considered limit, and 0 otherwise. Thus, the probability to have ignition of inflammable materials inside the building after blasting ($P(F/B)$) has been estimated through a lognormal distribution fitting (Fig 3.b).

The gypsum plasterboard with steel studs have been considered as internal partition between adjacent columns.Since the gypsum panels are used as insulation system, they can be considered as fireproof materials. Thus, each volume identified by two adjacent columns has been considered as fire compartment.
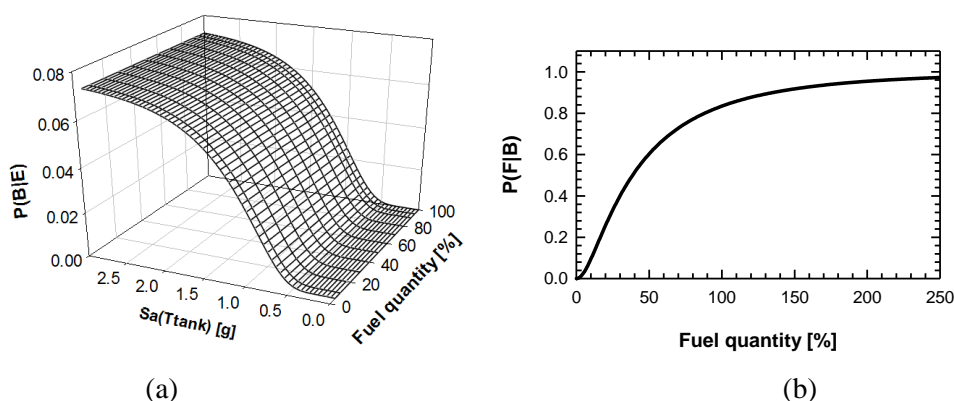

(a)   (b)

Fig 3 – Probability to have an explosion after the earthquake (a), and probability to have the fire after the blast (b)

4. Methods and models

4.1 Earthquake

The time history analyses have been performed on an appropriately modeled three-dimensional structure utilizing SAP2000 [14]. The lateral resisting system is a dual system. It is made up of moment resisting frames and braces, in both directions. The beams and columns have H sections, while hollowed structural section (HSS) have been assigned to the braces. The concentrated plasticity model has been used to take into consideration the nonlinearity of the structural elements. According to FEMA-356 [15], Steel-beams Flexural Hinge (type Moment M3) and Steel-column Flexural Hinge (type P-M2-M3 with M-χ cylindrical domain) has been used for beam and column elements, respectively. The plastic hinges for brace elements have been modeled as Steel-braces Axial Hinges. A 3% damping ratio has been assigned to the frames according to Rayleigh formulation. The nonlinear dynamic analyses have been performed using non-linear direct integration method, taking into account P-Δ effects and applying the horizontal acceleration time histories in the two principal directions of the building.

4.2 Blast

The U.S. Army Technical Manual (TM5-1300) [16] is a highly recognized standard which is used to estimate the basic parameters of blast load through a series of charts. Charts provided by TM5-1300 [16] have been used in this study in order to establish the blast load parameters required in structural analysis. Generally, the blast wave demand is expressed as a function of universal scaled distance parameter (Z) which is directly proportional to the equivalent weight of TNT (W_{TNT}) and inversely proportional to the stand-off distance of explosive relative to a particular target (R). TNT equivalent charge weight of LPG is given by Eq. (5) [17]:

$$W_{TNT} = \varepsilon \cdot \frac{\Delta H_{LPG} \cdot W_{LPG}}{\Delta H_{TNT}} \tag{5}$$

where W_{LPG} is weight of LPG, DH_{LPG} and DH_{TNT} are heat of combustion for LPG and TNT respectively, and e is a unit-less parameter to take in account the partial combustion and physical difference between TNT and gaseous explosion. In addition, the effect of tank shell has been considered by applying an empirical weight equivalency factor [22]. Twelve different fuel quantities (from5% to 100%) representative of different IMs for performing blast analyses have been considered in this study. To perform nonlinear time history analysis, the typical blast overpressure time history provided by TM5-1300 [16] has been applied. The blast time history overpressure has been idealized by rise of an equivalent triangular pulse of maximum reflected pressure (P_r) at an arrival time (t_A) after the explosion (Fig 4). A fictitious duration (t_{rf}) has been determined in place of the actual positive duration (t_o) assuming the linear decay of overpressure given by Eq. (6):

$$t_{rf} = 2i_r / p_r \tag{6}$$

where i_r is the reflected impulse and P_r is the maximum reflected pressure determined through the charts provided by TM5-1300. A similar procedure for the negative phase has been used whereas rise time of negative peak pressure has been considered equals to 0.25 to negative fictitious duration (t_{rf-}). The different blast pressure time histories specific to each structural member have been established corresponding to the different scaled distance parameter (Z) and potential charge weight for each blast IM.

The blast dynamic pressure has been applied to the beams, columns and exterior walls of the exposed structural area on the front face of the explosion. The reflection areas of the building have been assumed big enough in order that there is no blast wave diffraction around the structure. The exterior walls have been considered as typical concrete masonry wall reinforced with vertical bars. The wall components have been assumed as one-way spanning elements that can transfer only the equivalent reaction load to the adjacent beams. Each wall has been simplified to an equivalent SDOF system in such a way that the deflection of the concentrated mass to be same as the mid-span of the actual wall. An elasto-perfectly plastic behavior for

7

each wall has been defined and the dynamic characteristics have been adjusted for the condition of high-velocity impacts [16]. A MATLAB code has been used to calculate the dynamic responses of the mid-span of the wall considering the plastic hinge formation (yielding rotation capacity). Then, resulted time history reactions have been directly applied to the adjacent beams in SAP2000 models. Blast pressure time histories relevant to the beams and columns have been applied directly on the framing elements. In order to take into account the effects of high-rapid load environment, mechanical properties of steel materials have been enhanced by means of dynamic increased factor (DIF) [16]. Structural damping effects have been ignored since the blast load duration is short in compare to the natural period of the structure. The transmission of the ground shock induced by the explosion to the foundation of the structure has not been considered in this paper. Finally, twelve different nonlinear time history analyses have been conducted. In the cases of the loss of the load-bearing capacity of key structural elements, the progressive collapse analyses have been carried out and thus the dynamic effects of removal of the failed elements have been evaluated using time history analyses.
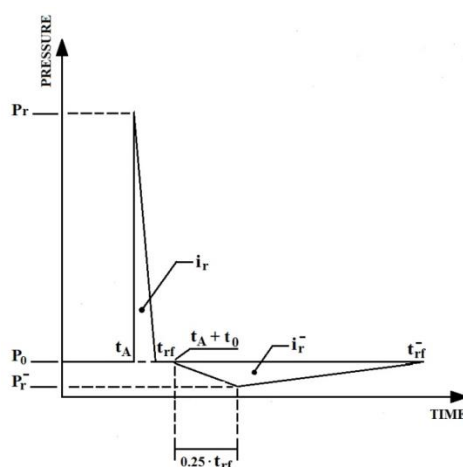

Fig 4 – Idealized blast overpressure time history (adopted from [16])

4.3 Fire

The ignition of inflammable materials within the compartment generates a flashover that will then cause a rise in temperature. The fire curve for the compartment is majorly used to determine the design-basis fire action. The fire curve is simply the evaluation of post-flashover time-temperature relationship and is determined by the quantity of combustible materials (total calorific value), the velocity of combustion, and the ventilation conditions. The quantity of combustible materials (total calorific value) and the velocity of combustion are main determinant of the entire heat flux that is produced inside the compartment (q_f). It is assumed that the compartment heat flux is normally distributed. The mean value and standard deviation are used to specify the exact fire load for different building category in accordance to EC1 [18]. The normal mean specific fire load and standard deviation for hospitals are 230 MJ/m^2 and 69 respectively. In the study case, the specific heat flux of the compartment has been selected as IM_2 and eight different exceedance probabilities (P_q) have been considered (Table 1).

Table 1 – Selected exceedance probability for the heat compartment flux.

P_q [%]	90	85	80	50	20	10	5	2
q_f [MJ/m^2]	135	160	180	230	281	322	360	400

The temperature-time relationship developed by Lie [19] has been considered. The peak temperature (T_{peak}) and peak time (t_{peak}) are both used to describe the top of the curve. The definition of these parameters has been done in accordance to the time equivalence concept, which is related to the actual fire exposure to

8

the standard test fire (standard curve). The ventilation factor *w*, is one of the main parameters used to evaluate the equivalent time. In the study case, two vertical openings having dimension of 1.50m×2.00m and opening factor of 0.07 have been considered. Table 2 resumes the major parameters of the temperature-time curves for each generated heat flux. An evaluation of the degradation of the physical and mechanical characteristics of the materials by fire has been conducted. In accordance to Fourier's equation, the net transmitted heat flux ($q_{f,n}$) is used to determine the thermal distribution for any fire scenario. In a system where the entire structural element is homogenous and isotropic, the Fourier's equation can be incorporated into the element's volume and then rephrase discretely to obtain Eq. (7) .

$$\Delta T_{(i)} = k_{sh} \cdot \frac{A_m / V}{\rho \cdot c} \cdot q_{f,n(i)} \cdot \Delta t \tag{7}$$

where $\Delta T_{(i)}$ is a definition of ith increment of uniform temperature in the cross section area of the element while A_m/V is the section factor given by the ratio between the area of the element exposed to fire (A_m) and its total volume (V). Density (ρ) and specific heat (c) refer to the materials that made up the structural element while Δt is the time it takes the change in temperature to take place ($\Delta t < 5s$). The coefficient k_{sh} is used to consider of the "shadow effects" that cause non-uniform thermal transversal distribution. In order to achieve a pseudo-uniform transversal temperature distribution, k_{sh} coefficient has been assessed as the actual fire exposure. Parameter $k_{sh}= 0.7$ has been considered for beams (fire exposure on three sides) while $k_{sh} = 0.9\lfloor (A_m / V)_b / (A_m / V) \rfloor$ has been assumed for columns.

Table 2 – Characteristic time-temperature curve parameters for each generated heat flux

P_q [%]	90	85	80	50	20	10	5	2
t_e [min]	23.50	25.00	26.19	33.46	40.83	46.85	52.2	58.2
T_{peak} [K°]	1111	1131	1145	1173	1188	1205	1218	1228
t_{peak} [min]	11.5	13.5	16	20.5	24.5	29.5	33.5	37

The element's section factor that is taken as bin section ratio is represented as $(A_m/V)_b$, while (A_m/V) represents the column's actual section factor.The fire exposure for the column has been supposed for one side of the web and for both flanges. Three different sections of beams and columns have been identified for the compartment. Fire resistance of steel elements inside the compartment has been assessed considering the maximum uniform thermal loads for each heat flux value. The analyses have been accomplished with the help of the software SAP2000. The mechanical and physical materials properties have been modified according to AISC depending on the temperature values. The nonlinearity of the structural elements has been taken into account according to concentrated plasticity model. Progressive nonlinear analyses have been performed. The nonlinearity effects have been taken into account in accordance to concentrated plasticity model. Progressive nonlinear analyses have also been carried out.

5. Structural analysis

5.1 Earthquake

Maximum transient inter-story drifts have been considered as EDP to assess the performance of the structure under the seismic load. Fragility curves, for both principal horizontal directions, have been investigated for the different damage states (slight, moderate, extensive, and complete) according to ATC P-58 [10] (Fig 5).
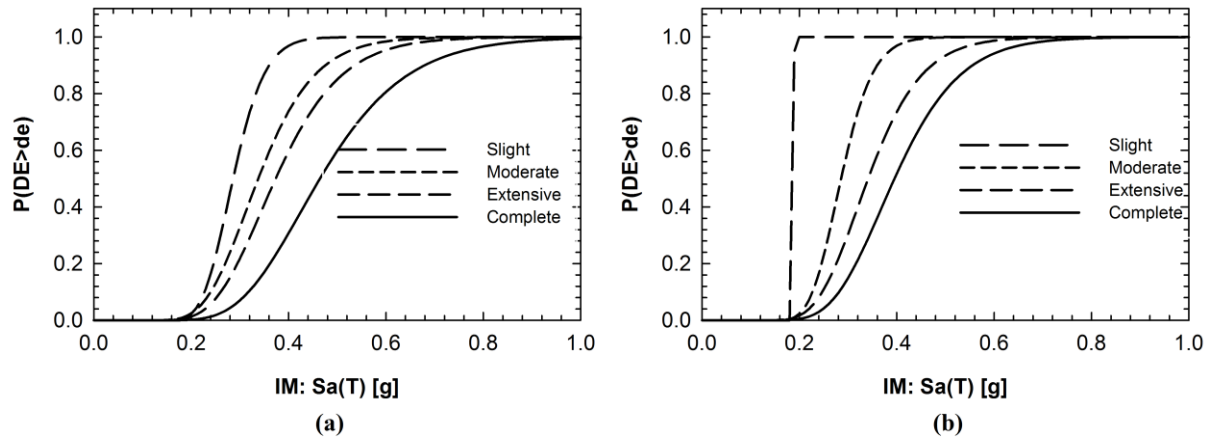
9

Fig 5 – Fragility curves in X direction (a) and Y direction (b) for earthquake hazard

5.2 Blast

An accurate assessment of the global response of building under blast load has been accomplished by assuming the loss of horizontal stiffness as EDP. In the Y direction, response of the structure is integrated into the SDOF dynamic response based on the specification of Eq. (8).

$$K_{eq} = \frac{\delta_{eq}}{V_{eq}} = \frac{\delta_{top} \cdot \sum_{i=1}^{N=5} (\phi_i - \phi_{i-1})^2}{V_b \cdot \sum_{i=1}^{N=5} \phi_i} \tag{8}$$

where d_{top} represents the maximum top floor displacement and V_b is the base shear obtained at the same time of the maximum displacement. In this case, the actual distribution of floor displacements has been taken into consideration and this usually occur through the shape coefficients ϕ_i, where i^{th} is associated to the floor displacement normalized with respect the top one. The yielding drift for braced system has been calculated according to ATC P-58 [10] and the maximum drift threshold have been assumed (Table 3) for four different damage states. The stiffness reduction limits have also been computed. The computation involves an assumption of an elastic-perfectly plastic global behaviour of the steel frame.Fig 6.a depicts the fragility curves for each DS.

Table 3 – Damage States for blast analysis

Damage State	Slight	Moderate	Extensive	Complete
Inter-story drift [%]	1.00	1.80	2.80	4.80
Stiffness reduction [%]	30.00	61.00	75.00	85.00

5.3 Fire

The assessment of structural capacity has been carried out evaluating the highest obtainable deflection for beams and columns as EDP. In this case, two different damage states have been considered that are (*i*) DS1 corresponding in an irreversible damage on the beam with maximum response; (ii) DS2 that consists in an irreversible damage in the column with maximum response. The first damage state provides useful data on the highest flexural capacity of the beam. It is assumed that the threshold vertical deflection (v_b) for this damage state is equivalent to deflection attributed to uncontrolled vertical displacement. The second damage

10

state is linked to the highest drift of the column (δ_c) which occurs under multiple stresses as a result of compression and bending moment and with full consideration of the P-Δ effects. It has been assumed that the drift's highest limit coincides with the horizontal displacement that generates uncontrollable unstable displacement. For each analysis, the probability to have irreversible damage to the structural elements has been assumed equal to 1 if the response parameter is greater than the associated limit and 0 otherwise. Fragility curves have been developed fitting lognormal distribution to the data (Fig 6.b).
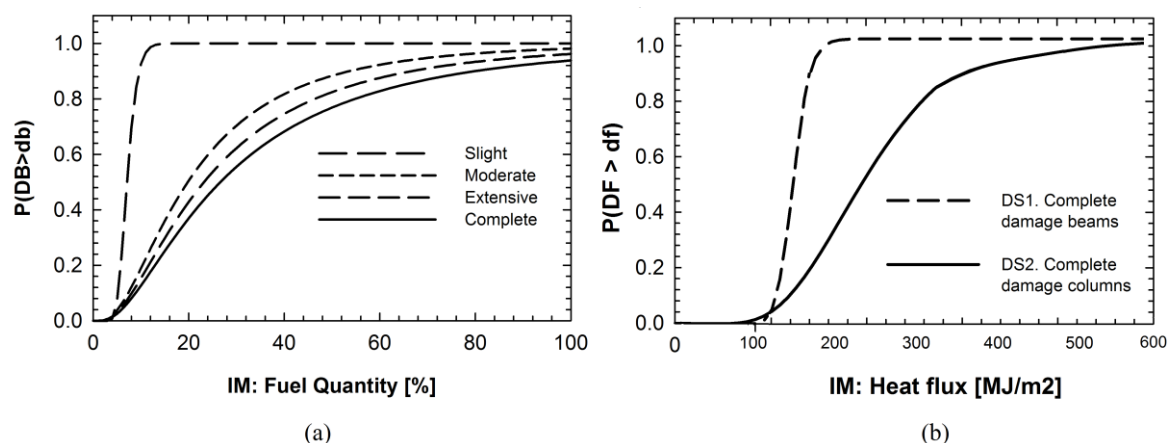

Fig 6 –Fragility curves for blast hazard(a), and fragility curves for fire hazard (b)

6. Conclusion

Recent accidents have revealed the vulnerability of buildings and infrastructures to multiple hazards. The combination of different hazards has to be considered to evaluate the performances of a building and the respective economic losses. The proposed methodology is able to estimate the cumulative structural damage probability due to sequential hazardous events for a given damage state. The hazards interaction is assessed by using various physical models. However, this new approach requires calibration of all necessary physical parameters, especially those that play important role in reducing the epistemic uncertainties of the model. Generally, small size tanks do not suffer extensive damage under strong ground motions. On the contrary, the seismic vulnerability of big size tanks (e.g. farm or industrial tanks) may result crucial. In these cases, the failure modes and the damage on the equipment indicate a large sensitivity to the seismic actions. In a context of multiple-hazard approach, each hazard must not be considered as independent phenomenon. The variation of the mechanical and physical parameters (chain effects) of the structural model strongly influences the cumulative damage estimation. For the proposed case study, assuming the three hazards as independent phenomena is a reasonable hypothesis, since the chain effects do not influence the total damage estimation. The application of the proposed multi-hazard approach can be used for both improving the structural safety and reducing the building life cycle costs to enhance the resilience of the structure [20].

7. Acknowledgements

8. Copyrights

9. References

[1] Delmonaco G, Margottini C, Spizzichino D (2006): ARMONIA methodology for multi-risk assessment and the harmonisation of different natural risk maps. *Deliverable 3.1. 1, ARMONIA*.

[2] Marasco S, Noori AZ, Cimellaro GP (2017): Cascading Hazard Analysis of a Hospital Building. *Journal of Structural Engineering, ASCE*, **143**(9), 04017100.

[3] Barbato M, Petrini F, Unnikrishnan VU, Ciampoli M (2013): Performance-based hurricane engineering (PBHE) framework. *Structural Safety*, **45**, 24-35.

[4] Asprone D, Jalayer F, Prota A, Manfredi G (2010): Proposal of a probabilistic model for multi-hazard risk assessment of structures in seismic zones subjected to blast for the limit state of collapse. *Structural Safety*, **32**(1), 25-34.

[5] Fabbrocino G, Iervolino I, Orlando F, Salzano E (2005): Quantitative risk analysis of oil storage facilities in seismic areas. *Journal of hazardous materials*, **123**(1-3), 61-69.

[6] Cimellaro GP, Malavisi M, Mahin S (2017): Using Discrete Event Simulation Models to Evaluate Resilience of an Emergency Department. *Journal of Earthquake Engineering*, **21**(2), 203-226.

[7] Cimellaro GP, Malavisi M, Mahin S (2018): Factor analysis to evaluate hospital resilience. *ASCE-ASME Journal of Risk and Uncertainty in Engineering Systems, Part A: Civil Engineering*, **4**(1), March 2018

[8] Boore DM, Atkinson GM (2008): Ground-motion prediction equations for the average horizontal component of PGA, PGV, and 5%-damped PSA at spectral periods between 0.01 s and 10.0 s. *Earthquake Spectra*, **24**(1), 99-138.

[9] Cimellaro GP, Marasco S (2015): A computer-based environment for processing and selection of seismic ground motion records: OPENSIGNAL. *Frontiers in Built Environment*, **1**, 17.

[10] Porter K, Kennedy R, Bachman R (2006): Developing fragility functions for building components for ATC-58. *A Report to ATC-58. Applied Technology Council, Redwood City, CA, US*.

[11] Code UB (1997): UBC-97, in *Structural engineering design provisions. International conference of building officials, Whittier, California*.

[12] Allen E (2015): Deepwater facility integrity management: a state-of-the-art review, in *SPE/IATMI Asia Pacific Oil & Gas Conference and Exhibition*. Society of Petroleum Engineers.

[13] Higham DJ, Higham NJ (2016): *MATLAB guide*. SIAM.

[14] SAP C (2007): Integrated software for structural analysis & design. *Computer and Structures. Inc. Berkeley*.

[15] Prestandard F (2000): commentary for the seismic rehabilitation of buildings (FEMA356). *Washington, DC: Federal Emergency Management Agency*, **7**.

[16] Army USDot (1991): *Structures to resist the effects of accidental explosions*. Vol. 88. Departments of the Army, Navy, and Air Force.

[17] Sutton S, McCauley E (1975): Assessment of hazards resulting from atmospheric propane explosions at LLL. California Univ., Livermore (USA). Lawrence Livermore Lab.

[18] Formichi P (2008): EN 1991–Eurocode 1: Actions on structures Part 1-3 General actions–Snow Loads, in *presentation at Workshop "Eurocodes. Background and Applications*. pp. 18-20.

[19] Lie TT (1974): Characteristic temperature curves for various fire severities. *Fire Technology*, **10**(4), 315-326.

[20] Cimellaro GP, Renschler C, Reinhorn AM, Arendt L (2016): PEOPLES: a framework for evaluating resilience. *Journal of Structural Engineering, ASCE*, **142**(10), 1-13 DOI: 10.1061/(ASCE)ST.1943-541X.0001514.